Biomaterials 34 (2013) 1942–1953

Contents lists available at SciVerse ScienceDirect

Biomaterials

journal homepage: www.elsevier.com/locate/biomaterials

The guidance of stem cell differentiation by substrate alignment and mechanical stimulation

Siddarth D. Subramony, Booth R. Dargis, Mario Castillo, Evren U. Azeloglu, Michael S. Tracey, Amanda Su, Helen H. Lu*

Biomaterials and Interface Tissue Engineering Laboratory, Department of Biomedical Engineering, Columbia University, New York, NY 10027, USA

ARTICLE INFO

Article history:
Received 7 September 2012
Accepted 10 November 2012
Available online 13 December 2012

Keywords:
Mesenchymal stem cell
Nanotopography
Biomimetic material
Bioreactor
Integrin
Ligament

ABSTRACT

Mesenchymal stem cells (MSC) represent a promising and clinically relevant cell source for tissue engineering applications. As such, guiding MSCs toward specific lineages and maintaining these phenotypes have been particularly challenging as the contributions of mechanical, chemical and structural cues to the complex differentiation process are largely unknown. To fully harness the potential of MSCs for regenerative medicine, a systematic investigation into the individual and combined effects of these stimuli is needed. In addition, unlike chemical stimulation, for which temporal and concentration gradients are difficult to control, mechanical stimulation and scaffold-based cues may be relatively more biomimetic and can be applied with greater control to ensure fidelity in MSC differentiation. The objective of this study is to investigate the role of nanofiber matrix alignment and mechanical stimulation on MSC differentiation, focusing on elucidating the relative contribution of each parameter in guided regeneration of functional connective tissues. It is observed that nanofiber alignment directs MSC response to physiological loading and that fibroblastic differentiation requires a combination of physiologically-relevant cell–material interactions in conjunction with mechanical stimulation. Importantly, the results of this study reveal that systemic and readily controllable cues, such as scaffold alignment and optimized mechanical stimulation, are sufficient to drive MSC differentiation, without the need for additional chemical stimuli. Moreover, these findings yield a set of fundamental design rules that can be readily applied to connective tissue regeneration strategies.

1. Introduction

Mesenchymal stem cells (MSC) have the ability to differentiate into chondrocytes [1], osteoblasts [1], adipocytes [1] and ligament or tendon fibroblasts [2]. These cells, which can be routinely harvested via bone marrow biopsy [1], readily proliferate and respond to multiple stimuli, including chemical [1] and mechanical [2]. They are also essential for wound healing and connective tissue repair [3], giving rise to differentiated cell types that are directly responsible for new tissue formation [3–5], with likely a combination of structural, chemical and mechanical cues directing this process. In addition to being critical for tissue repair, MSCs are also an ideal cell source for regenerative medicine [6]. In the tissue engineering paradigm, a scaffold, in conjunction with a cell source, guide tissue formation and enable tissue regeneration [7]. While differentiated cells have largely been used to test this approach, MSCs are considered a more realistic and optimal cell source due to their versatility and translatability. However, consistently guiding MSCs toward specific lineages remains a challenge, with significant variability in MSC cultures in terms of proliferation, differentiation capacity and senescence [8]. As a result, there is a need to elucidate the local (*e.g.* matrix environment) and systemic (*e.g.* mechanical and chemical) cues that guide MSC induction, in order to maintain the fidelity of differentiated MSC and enable their clinical translation.

Nanofiber-based scaffolds have been investigated for the regeneration of connective tissues, such as bone [9,10], meniscus [11], intervertebral disk [12], cartilage [13], tendons and ligaments [14–16], as they are biomimetic and can be fabricated to replicate the structural organization of the collagenous matrix that dominates these tissues. Moreover, nano-scale fibers have been shown to direct cell attachment and matrix deposition [14,17–20] and represent an ideal system to model the collagenous matrices present within native tissue structures. These scaffolds exhibit high aspect ratio, surface area, permeability and porosity, and can be fabricated from a variety of polymers, both natural and synthetic, with tunable fiber diameter and matrix alignment [21,22].

* Corresponding author. Department of Biomedical Engineering, Columbia University, 1210 Amsterdam Avenue, 351 Engineering Terrace, MC 8904, New York, NY 10027, USA. Tel.: +1 212 854 4071 (office); fax: +1 212 854 8725.
E-mail address: hhlu@columbia.edu (H.H. Lu).

0142-9612/$ – see front matter © 2012 Elsevier Ltd. All rights reserved.
http://dx.doi.org/10.1016/j.biomaterials.2012.11.012

Given their similarity to the native extracellular matrix (ECM), nanofiber-based scaffolds have been used to promote MSC response and differentiation. For example, Ma *et al.* demonstrated that poly(L-lactic) acid (PLLA) nanofiber alignment increased the calcium production of rat MSC in conjunction with osteogenic medium [23]. Similarly, Baker *et al.* reported that for bovine MSCs on poly(ε-caprolactone) (PCL) nanofibers, a greater increase in scaffold mechanical properties was measured on aligned nanofibers after 10 weeks when coupled with chondrogenic induction medium [11]. Notably, the majority of these studies have employed chemical factors along with scaffold cues, making it difficult to decouple the effects of these distinct stimuli [24]. However, recent studies by Schofer *et al.* [25] and Jiang *et al.* [26] demonstrate that nanofiber architecture alone may guide MSC differentiation.

In addition to matrix-guided cues, mechanical stimulation has been found to direct MSC differentiation [2,27,28]. For example, Altman *et al.* demonstrated that dynamic tensile (10%) and torsional (25%) strains applied at 1 cycle/minute upregulated types I and III collagen expression by human MSCs in collagen gels and directs these cells toward a fibroblastic phenotype without the use of exogenous growth factors [2]. Similarly, recent studies have also demonstrated the potential of compressive strain [27] and shear flow [28] for cartilage and bone tissue engineering, respectively, when coupled with induction media.

Collectively, these findings suggest that mechanical loading and scaffold nano-architecture are important in guiding MSC differentiation. However, published work evaluating the effect of either nano-scale cues or mechanical loading on MSC differentiation have largely been conducted in the presence of induction media, making it difficult to identify the precise impact of each factor alone. Moreover, the interactive effects of physiological loading and matrix alignment have not been determined for MSCs. Therefore, the purpose of this study is to investigate the role of nanofiber matrix alignment and mechanical stimulation on MSC differentiation, focusing on elucidating the relative contribution of each parameter in guided regeneration of functional connective tissues.

Using the anterior cruciate ligament (ACL), the most frequently injured ligament in the knee, as a model system, this study will evaluate the fibroblastic differentiation of human MSCs on nanofiber scaffolds as a function of fiber alignment and mechanical stimulation. Mesenchymal stem cells represent an optimal cell source as primary ACL fibroblasts, due to a lack of available donor tissue from which to obtain cells, are not feasible for ligament tissue engineering. This is the first study, to our knowledge, that seeks to decouple the effects of substrate alignment and mechanical stimulation on human MSC differentiation. It is hypothesized that tensile stimulation combined with a biomimetic nano-scale substrate will direct MSC differentiation toward a ligament fibroblast-like phenotype and the subsequent production of a ligament-like matrix. To test this hypothesis, the attachment, proliferation, biosynthesis and differentiation of MSCs stimulated by dynamic tensile loading will be evaluated on aligned and unaligned nanofiber scaffolds over a four-week culturing period. It is expected that the results of this study will elucidate fundamental substrate and culture environment-related rules that can be used to systematically control MSC differentiation, and determine whether loading or matrix alignment is the primary determinant of cell behavior, without confounding effects from concurrent chemical stimulation.

2. Materials and methods

2.1. Nanofiber scaffold fabrication

Unaligned and aligned nanofiber scaffolds composed of poly(lactide-*co*-glycolide) (PLGA, 85:15, M_w = 123.6 kDa; Lakeshore Biomaterials, Birmingham, AL) were produced via electrospinning [14,29]. Briefly, 35% PLGA (v/v) was solubilized in 55% N,N-dimethylformamide (Sigma–Aldrich, St. Louis, MO) and 10% ethyl alcohol. The solution was loaded into a syringe with an 18.5-gauge stainless steel blunt tip needle and electrospun at 8–10 kV and 1 mL/h using a custom electrospinning device. Polymer was dispensed via a syringe pump (Harvard Apparatus, Holliston, MA; 1 ml/h) and unaligned scaffolds were fabricated using a static collector plate whereas the aligned scaffolds were produced by electrospinning onto rotating mandrel (20 m/s). With the exception of fiber alignment, the resultant scaffolds were identical with respect to fiber diameter, pore size and porosity [14].

2.2. Cells and cell culture

Human mesenchymal stem cells (MSC, 21 y/o M) were obtained commercially (Lonza, Walkersville, MD) and maintained in culture with fully supplemented (FS) DMEM containing 10% FBS (stem cell certified, Atlanta Biologicals, Atlanta, GA), 1% penicillin-streptomycin, 1% non-essential amino acids, 0.1% amphotericin B and 0.1% gentamicin. Cells were cultured to 80% confluence and then passaged using 0.25% trypsin/1 mM ethylenediaminetetraacetate (EDTA) and re-plated at a density of 5×10^3 cells/cm^2. Cells from passage two were seeded on scaffolds for all studies. Prior to cell seeding, the stemness of these cells was ascertained using flow cytometry (BD FACSCalibur, Franklin Lakes, NJ) to confirm characteristic MSC surface markers, with cells determined to be positive for markers CD29, CD71, CD106 (BD Biosciences) and negative for markers CD14, CD31 and CD34 (BD Biosciences).

Scaffolds were secured in a custom high-throughput bioreactor (Fig. 1) to apply uniaxial tensile strain. Bioreactor translation of scaffold-level strain to the cells was verified following the methods of Nathan *et al.* [30] in which image analyses were used to measure cellular deformation and compare it to the applied strain. It was determined that the applied strain is linearly translated to cellular deformation on both the unaligned and aligned nanofibers (Fig. 1). A physiologically relevant loading regimen [31], consisting of 1% strain at 1 Hz for 90 min twice daily (10.5 h rest between cycles) was selected based on previous work that has shown that physiologic to sub-physiologic levels of strain are optimal for in vitro tissue formation at a cycle frequency of 1 Hz [32] as well as the established need for a rest period between strain cycles to maintain cell mechanosensitivity [33,34]. In addition, a pilot study was conducted to determine the optimal duty cycle. It was observed that loading at two cycles per day resulted in the highest cell number and total collagen by day 3 (Fig. 1).

In this study, electrospun scaffolds (5 × 6 cm) were sterilized via ultraviolet irradiation (15 min/side). Scaffolds were secured in loading cartridges via teflon clamps, sectioned into 5 cm × 1 cm strips and pre-incubated in FS medium at 37 °C and 5% carbon dioxide for 16 h. Cells were seeded on the scaffolds at a density of 3×10^4 cells/cm^2 and allowed to attach for 15 min before the addition of FS DMEM. Following an initial five-day period of static culture to allow for cell attachment and matrix production, the effects of mechanical stimulation on MSC morphology, attachment, proliferation, gene expression and matrix production were determined after 1, 7, 14 and 28 days of mechanical stimulation. Aligned and unaligned scaffolds cultured in identical bioreactor cartridges without loading served as controls.

2.3. Cell attachment and alignment

Cell attachment and alignment were imaged via scanning electron microscopy (SEM, 1.0 kV, Hitachi S-4700, Pleasanton, CA). Following fixation, samples were dehydrated in an ethanol series and then sputter-coated with gold-palladium to reduce charging effects.

Cell viability and morphology (n = 3/group) were evaluated using Live/Dead staining (Invitrogen, Carlsbad, CA) following the manufacturer's suggested protocol. The samples were imaged under confocal microscopy (Leica Microsystems TCS-SP5, Bannockburn, IL) at excitation wavelengths of 488 nm and 594 nm. Cell penetration was evaluated by taking a z-series of confocal images over a depth of 20 μm, equivalent to 15 to 20 layers of nanofibers.

The effects of mechanical loading and scaffold architecture on MSC alignment were quantified following the methods of Costa *et al.* [36] Briefly, confocal images (n = 3/group) of cell-seeded scaffolds were analyzed using circular statistics software customized for evaluating fiber alignment (Fiber 3).

2.4. Cell proliferation

Total DNA content was measured using the PicoGreen dsDNA assay (Invitrogen). At each time point, the samples (n = 5/group) were homogenized in 0.1% Triton-X (Sigma–Aldrich) and subjected to 20 s of ultrasonication at 5W. Fluorescence was measured using a microplate reader (Tecan, Research Triangle Park, NC) at an excitation wavelength of 485 nm and an emission wavelength of 535 nm. A standard curve was derived and used to correlate DNA concentration to fluorescence intensity, and cell number was determined based on a conversion factor of 8 pg DNA/cell [35].

2.5. Cell biosynthesis

Total collagen content per sample (n = 5/group) was calculated using the hydroxyproline assay. The assay was performed following a 16 h sample digestion in

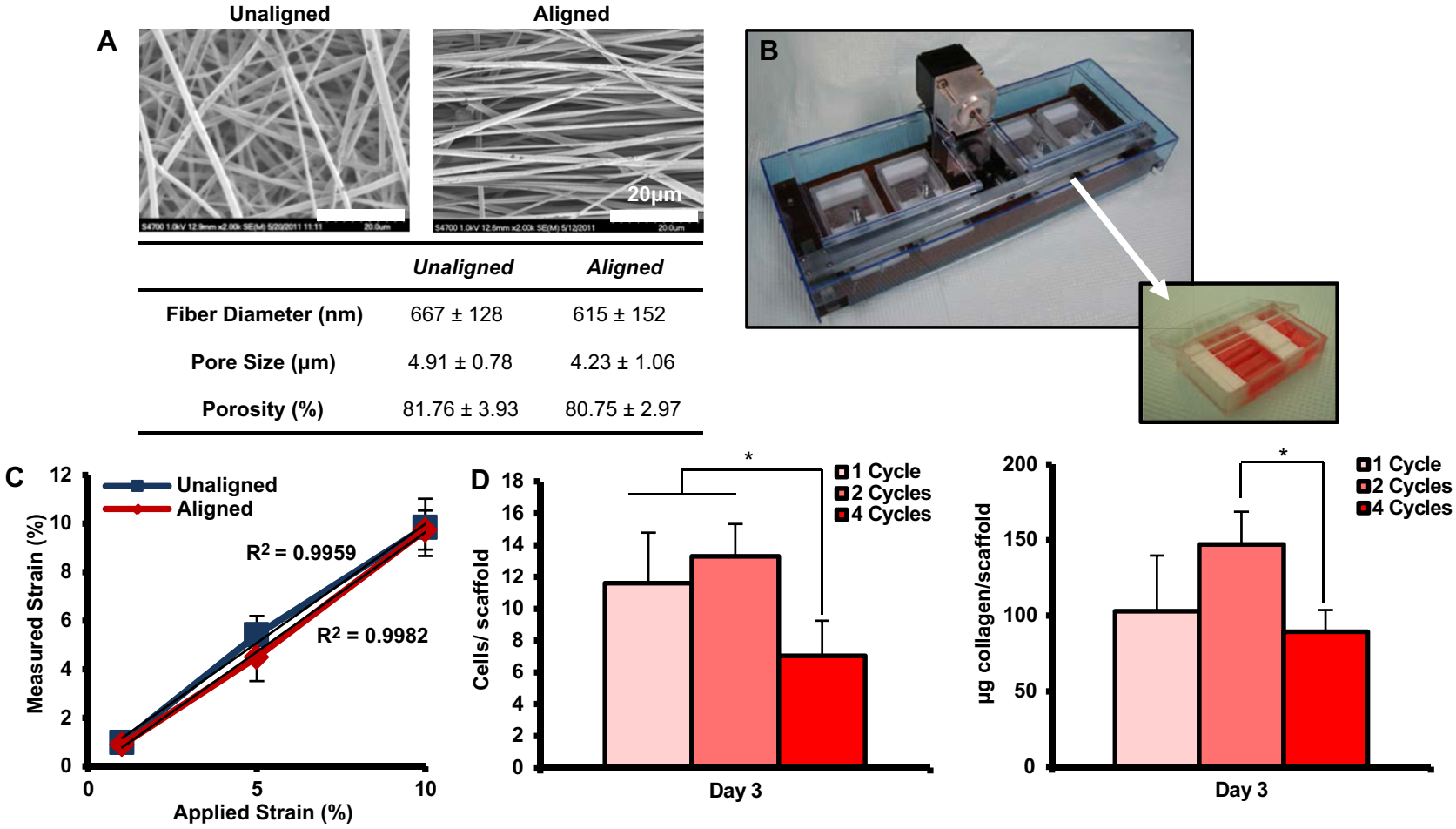

	Unaligned	*Aligned*
Fiber Diameter (nm)	667 ± 128	615 ± 152
Pore Size (μm)	4.91 ± 0.78	4.23 ± 1.06
Porosity (%)	81.76 ± 3.93	80.75 ± 2.97

Fig. 1. Modular bioreactor system for applying tensile strain to nanofiber scaffolds. A) Scanning electron micrographs of unaligned and aligned PLGA nanofiber scaffolds. B) Scaffolds are cultured in a custom bioreactor and load is applied via a linear actuator and stepper motor. Five nanofiber scaffolds are cultured in each individual bioreactor (inset) and the apparatus is housed within a cell culture incubator for the duration of the culture period. C) The bioreactor system was validated by applying strain to scaffolds and measuring cellular deformation via image analyses. It was demonstrated that measured strain linearly correlated with applied strain. D) The loading regimen duty cycle was optimized by performing a preliminary study evaluating 1, 2, and 4 cycles of loading per day. It was shown that highest cell number and collagen content was measured with the two cycle per day regimen after three days.

Papain (Sigma–Aldrich) to solubilize matrix proteins. Absorbance was measured using a microplate reader (Tecan) at 555 nm. A standard curve was generated and used to correlate total collagen content to absorbance.

Collagen distribution was also visualized using picrosirius red staining of frozen sections ($n = 2$/group). Briefly, after fixation, samples were embedded in 5% polyvinyl alcohol (PVA, Sigma–Aldrich) and 7 μm thick sections (spanning the depth and width of the scaffold) were obtained using a cryostat (Hacker-Bright OTF model, Hacker Instruments and Industries, Winnsboro, SC). Collagen distribution was visualized with picrosirius red staining under light microscopy (Axiovert 25, Zeiss).

Elaboration of type I and type III collagen ($n = 3$ samples/group) on scaffolds was evaluated using immunohistochemistry. After rinsing with PBS, samples were fixed with 10% neutral buffered formalin for 24 h. Monoclonal antibodies for type I collagen (1:20 dilution in serum-free Protein Block, Dako Cytomation, Carpinteria, CA) and type III collagen (1:100 dilution in serum-free Protein Block) were obtained from Abcam (Cambridge, MA) and Sigma–Aldrich, respectively. Samples were treated with 1% hyaluronidase for 30 min at 37 °C and incubated with primary antibody overnight. After a PBS wash, Alexa Fluor 488-conjugated secondary antibody (Invitrogen) was added and incubated for 1 h. Propidum iodide (Invitrogen) was used as a nuclear counterstain. Images were obtained using a confocal microscope (Leica TCS SP5) with 488 nm and 594 nm excitation wavelengths.

2.6. Fibroblastic markers

Gene expression ($n = 5$/group) was measured using quantitative real-time reverse transcriptase polymerase chain reaction (qPCR). Total RNA was isolated using the TRIzol (Invitrogen, Carlsbad, CA) extraction method. The isolated RNA was reverse-transcribed into cDNA via the SuperScript III First-Strand Synthesis System (Invitrogen) following the manufacturer's suggested protocol. The cDNA product was amplified and quantified through real-time PCR using SYBR Green Supermix (Invitrogen). Expression of fibroblastic markers type I collagen, type III collagen, fibronectin, tenascin-C, tenomodulin and scleraxis [54] as well as integrins α2, αV, α5 and β1 was determined. GAPDH served as the house-keeping gene (primer sequences listed in Table 1). All reactions were run for 50 cycles using the iCycler iQ Real-Time PCR Detection System (BioRad). Normalized expression levels reported were calculated based on difference between threshold cycles, namely, the difference in threshold cycle values between the gene of interest and the housekeeping gene GAPDH.

2.7. Statistical analysis

Results are presented in the form of mean ± standard deviation, with n equal to the number of samples per group. Two-way ANOVA was used to determine the effects of loading and time on cell alignment, proliferation, gene expression and matrix deposition. The Tukey–Kramer post-hoc test was used for all pair-wise comparisons and significance was attained at $p < 0.05$. Statistical analyses were performed with JMP IN (4.0.4, SAS Institute, Inc., Cary, NC).

3. Results

3.1. Cell attachment and alignment

The MSCs were cultured on aligned and unaligned nanofiber scaffolds in a custom designed loading bioreactor (Fig. 1). It was observed that cells remained viable and proliferated on both aligned and unaligned scaffolds. On unaligned scaffolds, a significantly greater number of cells were measured after 28 days of loading (Fig. 2). Similarly, significantly more cells were found on loaded aligned scaffolds by day 7, with cell number plateauing after 28 days. In terms of cell attachment, on unaligned scaffolds, as expected, random orientation of cells was observed without loading and this cell morphology was maintained over time. Interestingly, with loading, the cells adopted a markedly different morphology and aligned in the direction of applied strain by day 28. In contrast, a characteristic elongated fibroblast-like morphology was maintained on aligned scaffolds with no change observed due to either mechanical loading or culture duration.

To further investigate these apparent differences between groups, cell alignment on loaded and unloaded scaffolds was quantified using circular statistical analysis, focusing on changes in mean vector angle (MVA), angular deviation (AD) and mean vector length (MVL) [14,36] (Fig. 3). In general, values for the MVL range from 0 to 1, with the upper bound indicating greater horizontal alignment whereas the MVA ($-90° \leq \theta \leq 90°$) represents the angle of cells with respect to the horizontal axis, with a lower angle indicating horizontal alignment. Values for AD characterize the dispersion of the non-Gaussian angle of distribution (0–40.5°) with 0° representing horizontal alignment and 40.5° indicating random distribution. In this study, it was observed that on unaligned scaffolds, loading resulted in a significantly greater MVL (loaded: 0.94; unloaded: 0.33) and a significant decrease in AD after 28 days of culture as well as a distinct cell alignment profile ($p < 0.05$), represented as a histogram of cell orientation measured in each group (Fig. 3), all indicating a greater degree of horizontal alignment with respect to the unloaded group. In contrast, on aligned scaffolds, no difference in the MVL (0.91 vs. 0.93) or AD (11.74° vs. 9.21°) was found between the unloaded and loaded group.

3.2. Matrix deposition

In terms of collagen production (Fig. 4), on both aligned and unaligned scaffolds, a significant increase in total collagen content was found after 28 days of loading. Further analysis revealed that on a per-cell basis, mechanical loading upregulated cellular biosynthesis on both unaligned and aligned scaffolds, with significantly greater collagen production per-cell measured for both groups after 28 days of loading when compared to unloaded controls. Moreover, immunohistochemistry revealed that, independent of loading, the matrix formed on unaligned scaffolds consisted primarily of type I collagen. Similarly, a predominantly type I collagen matrix was seen on aligned scaffolds in the absence of loading. Interestingly, upon the application of loading, a matrix of both types I and III collagen was produced by the cells only on aligned scaffolds while the matrix deposited on the unaligned scaffolds remained predominantly of type I collagen.

3.3. Cell Differentiation

To further ascertain MSC differentiation, markers characteristic of the ligament fibroblast phenotype, including types I and III collagen, fibronectin, tenascin-C, scleraxis and tenomodulin, were assessed

Table 1
Gene primer sequences of fibroblast-related markers for quantitative real time RT-PCR.

Gene	Sense	Anti-Sense	Blast product Size(bp)
GAPDH	5'- GGCGATGCTGGCGCTGAGTA-3'	5'-ATCCACAGTCTTCTGGGTGG-3'	306
Collagen I	5'-TGGTCCACTTGCTTGAAGAC-3'	5'-ACAGATTTGGGAAGGAGTGG-3'	118
Collagen III	5'-GGCTACTTCTCGCTCTGCTT-3'	5'-CATATTTGGCATGGTTCTGG-3'	130
Fibronectin	5'-TTGAACCAACCTACGGATGA-3'	5'-AAATGACCACTTCCAAAGCC-3'	137
Tenascin-C	5'-TGCCCATTACAGGAGGTACA-3'	5'-CACTTTCCTCAAAGCCCTTC-3'	132
Scleraxis	5'-CAGCGGCACACGGCGAAC-3'	5'-CGTTGCCCAGGTGCGAGATG-3'	163
Tenodmoulin	5'-TTTGAGGAGGAGGGAGAAGA-3'	5'-TTCCTCACTTGCTTGTCTGG-3'	129
α2	5'-CAGAATTTGGAACGGGACTT-3'	5'- CAGGTAGGTCTGCTGGTTCA-3'	333
αV	5'-GATGGACCAATGAACTGCAC-3'	5'-TTGGCAGACAATCTTCAAGC-3'	207
α5	5'-GTGGCCTTCGGTTTACAGTC-3'	5'-AATAGCACTGCCTCAGGCTT-3'	181
β1	5'-GAGGAATACAGCCTGTGGGT-3'	5'-ATTGCAGGATTCAGGGTTTC-3'	121

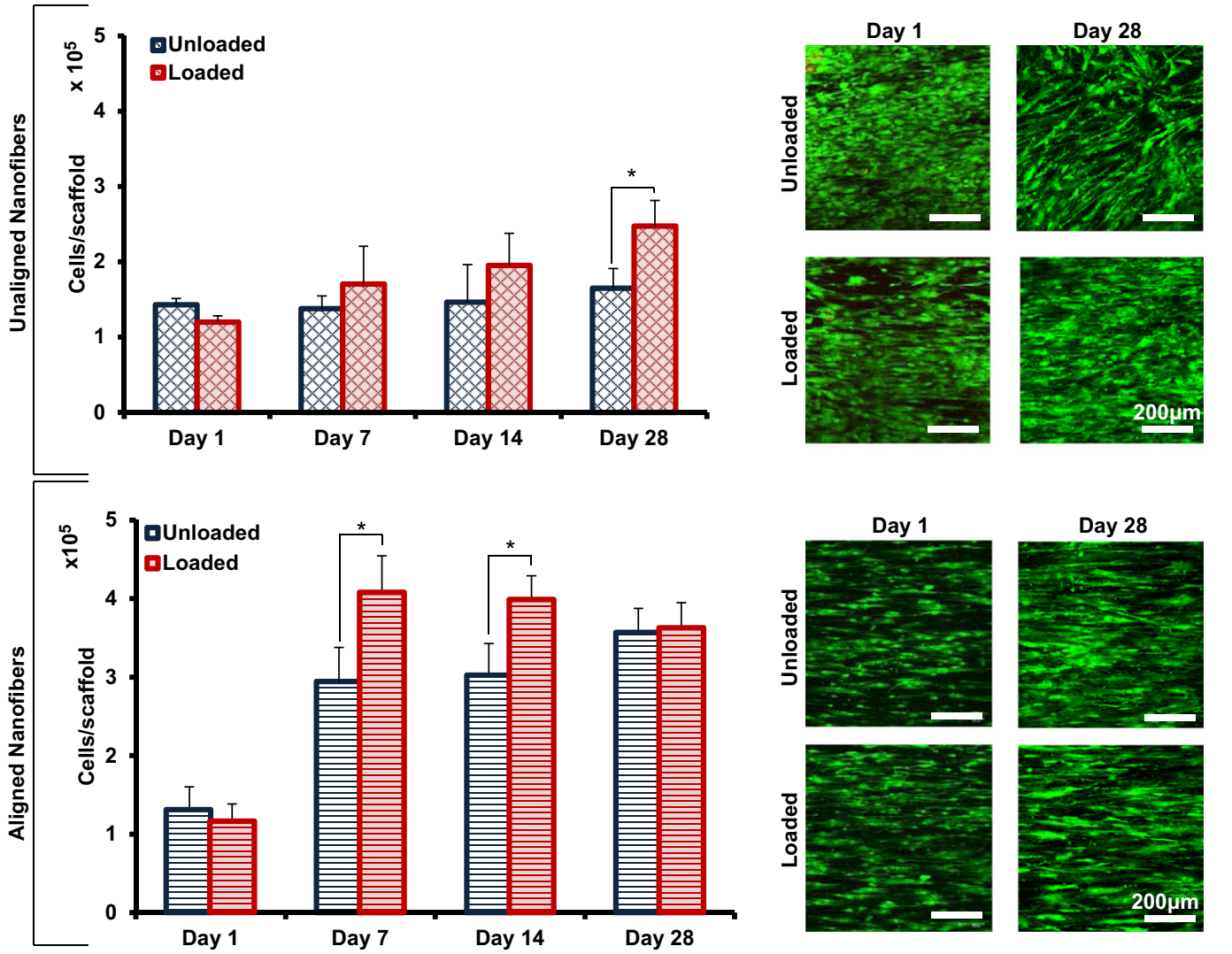

Fig. 2. *Cell Attachment and Proliferation.* On unaligned scaffolds, a significantly greater number of MSC were found after 28 days of loading. Cells attachment conformed to the underlying scaffold architecture in the unaligned group but appeared to align in the direction of loading with mechanical stimulation. On aligned scaffolds, an increase in total cell number was observed after seven days with equal numbers of cells present after 28 days. Cell morphology was similar both with and without loading.

using qPCR. On unaligned scaffolds, a mean increase in type I collagen was observed after seven days of loading and expression remained elevated after 28 days. The expression of type III collagen increased significantly (6.1 ± 1.0 fold higher with respect to the unloaded control) after seven days of loading but returned to control levels by day 28. Fibronectin expression was significantly upregulated after 14 days (2.0 ± 1.2 fold increase relative to unloaded control) and remained upregulated after 28 days in the loaded group. Notably, key fibroblastic markers tenascin-C, scleraxis and tenomodulin remained at basal level and were not upregulated by loading over time on unaligned scaffolds (Fig. 5). In contrast, on aligned scaffolds, type I collagen expression remained statistically similar both between groups and over time, although a three-fold increase in mean expression was observed after 28 days of loading compared to the unloaded group. Expression of type III collagen (4.1 ± 1.1 fold increase relative to unloaded control), fibronectin (5.1 ± 1.2 fold increase relative to unloaded control) and tenascin-C (4.3 ± 1.0 fold increase relative to unloaded control) was significantly upregulated after 14 days of mechanical stimulation, with the higher expression levels maintained after 28 days of loading. (Fig. 4). While no change in tenomodulin expression was observed over time on aligned scaffolds regardless of loading, scleraxis was downregulated after 28 days of static culture whereas its expression was maintained over time in the loaded group (Fig. 6). In addition, phenotype specificity was evaluated by measuring the expression of various osteogenic (Runx-2, osteocalcin) and chondrogenic markers (sox9, type II collagen). No upregulation of any of these markers was observed over time or with loading on either unaligned or aligned scaffolds.

3.4. Integrin Expression

Next, to better understand the mechanisms behind MSC mechanotransduction and the observed cell–matrix interactions, the expression of key integrins (α2, αV, α5, β1) was assessed as these surface-membrane receptors have been shown to mediate cell response to physical stimulation and matrix alignment [14,37–41]. It was observed that on unaligned scaffolds, both α2 and β1 were upregulated after 14 days of loading and expression levels were maintained thereafter, while the expression of α5 became significantly higher after seven days and plateaued thereafter (Fig. 6). On the aligned scaffolds, similar to the response on unaligned scaffolds, αV expression did not change in response to loading. However, distinct expression profiles, as compared to the unloaded control, were measured with integrin subunits α2, α5 and

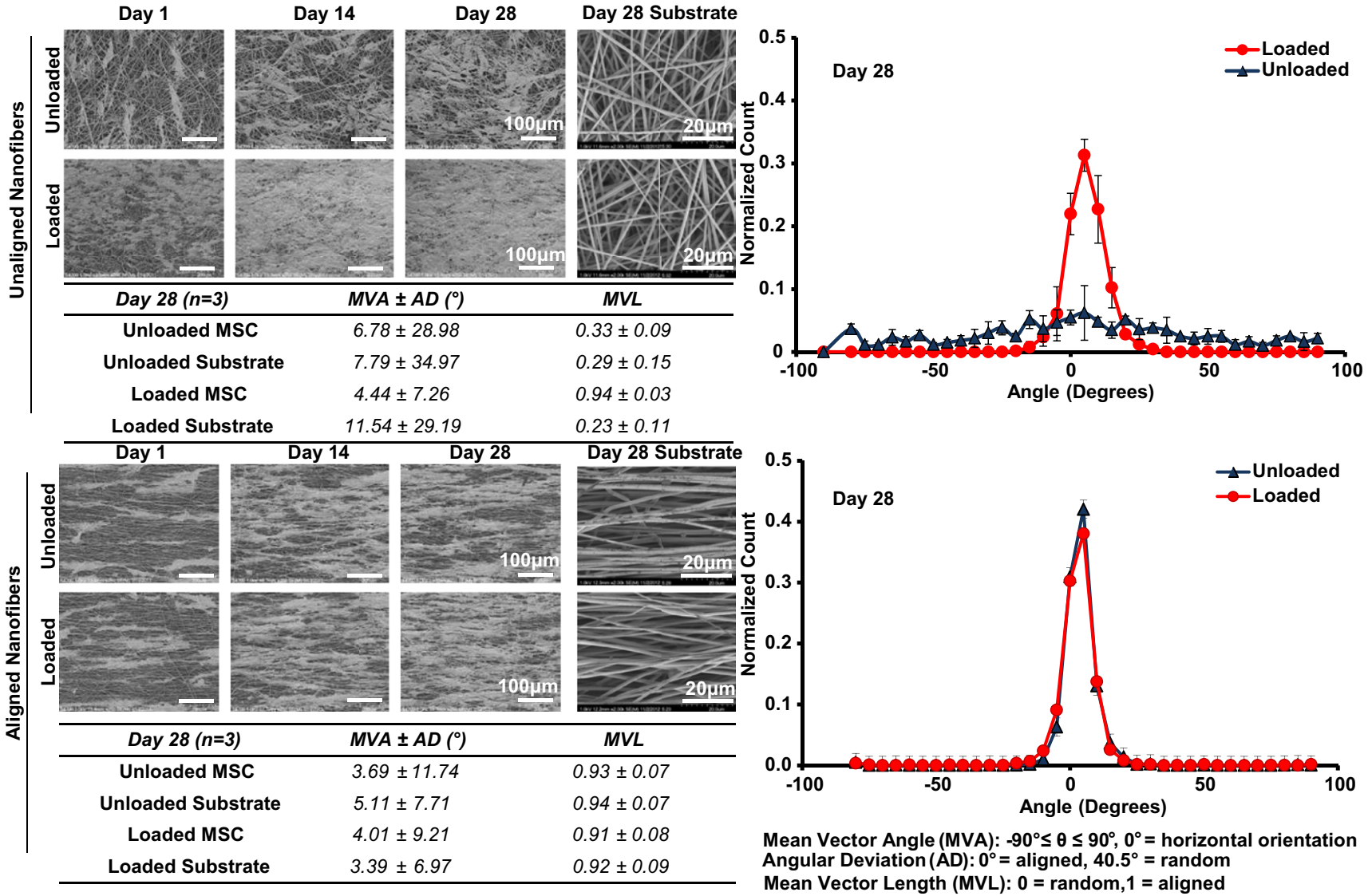

Fig. 3. *Cell Alignment*. A distinct difference in MSC alignment was observed on unaligned scaffolds after 28 days of loading with cells predominantly aligned in the direction of loading on strained scaffolds, as quantified via circular statistical analysis. Analysis via SEM indicated that cells spanned across fibers as opposed to following individual fibers. No difference in either substrate or cell alignment was observed on aligned scaffolds due to loading.

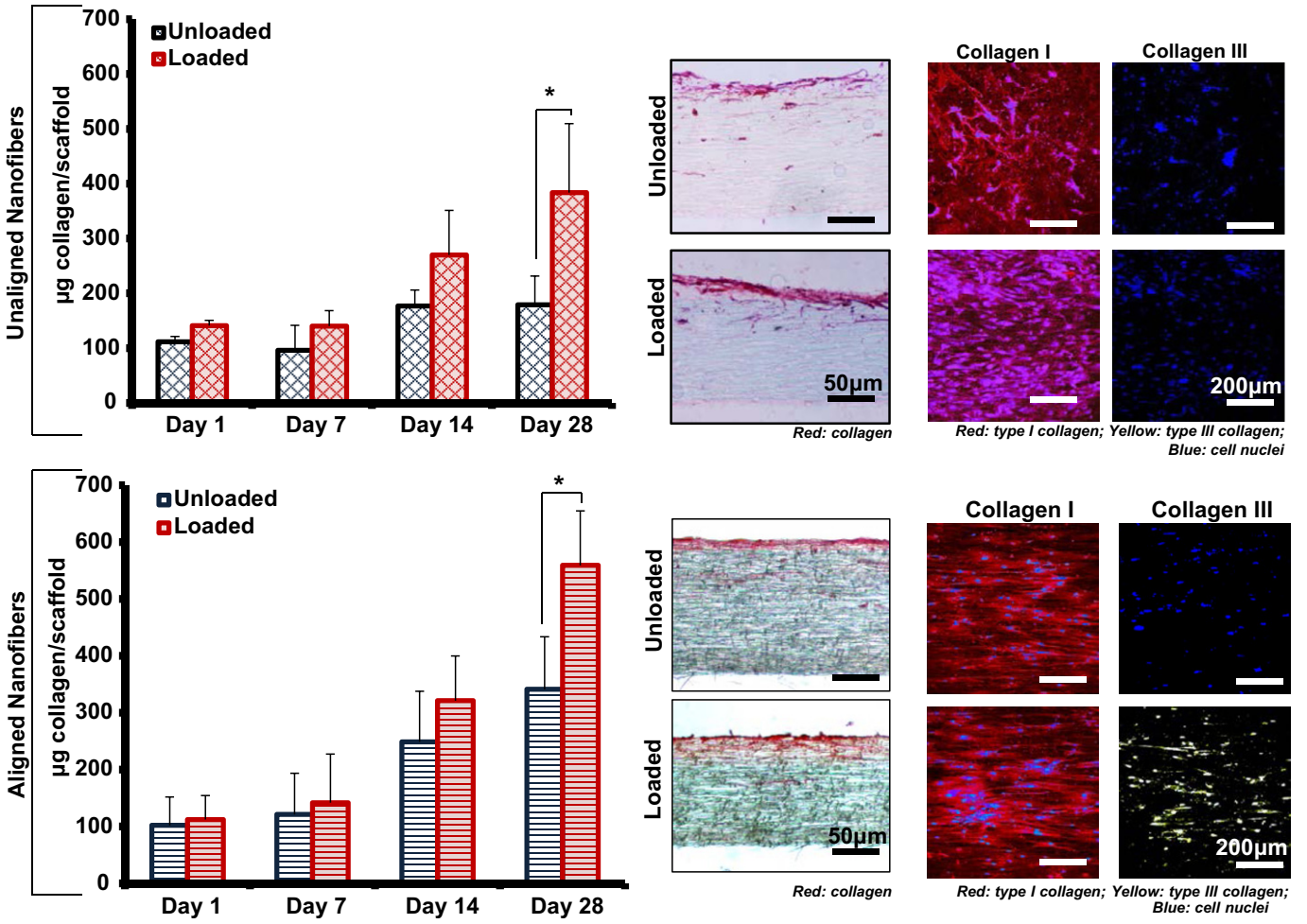

Fig. 4. *Cell Matrix Deposition*. A significant increase in total collagen was measured in both aligned and unaligned groups after 28 days of dynamic loading. Immunohistochemistry after 28 days of culture revealed that the matrix was primarily composed of type I collagen on unaligned scaffolds while both type I and III collagen were deposited on aligned scaffolds subjected to mechanical loading.

β1 being upregulated after 14 days of culture, and expression levels were maintained after 28 days on the loaded scaffolds ($p < 0.05$, Fig. 6).

4. Discussion

The objective of this study is to investigate the role of nanofiber alignment and mechanical stimulation on MSC differentiation, focusing on elucidating the relative contribution of each parameter as well as their interaction. The effect of substrate alignment, loading as well as the combination of the two factors is summarized in Table 2. It is observed that fibroblastic differentiation of MSCs is only possible when cultured on aligned nanofibers and co-stimulated with tensile loading. In contrast, when loading is applied to MSCs on unaligned scaffolds, cells fail to undergo fibroblastic differentiation and do not deposit a ligament-like matrix, despite adapting their morphology to align in the direction of loading. These findings provide the first evidence that there is an interactive effect between matrix alignment and mechanical loading, and that in the absence of chemical induction, co-stimulation is required for the induction of MSC differentiation into fibroblasts.

In terms of cell alignment and morphology, cells aligned in the direction of strain on the unaligned scaffolds whereas no change in alignment occurred over time on the aligned scaffold in response to tensile stimulation. These findings suggest that the underlying nanofiber organization is the primary determinant of cellular alignment and that contact guidance drives long-term cellular organization. However, similar to fibroblasts grown on non-patterned substrates [42,43], cell alignment can also be modulated by exogenous factors, such as the direction of applied strain, to orient them in a more physiologically relevant arrangement. For cell growth, the significant increase in cell number on unaligned scaffolds in response to loading, despite similar numbers of initially seeded cells on both the unloaded and loaded groups, may be due to a greater cell density achieved with linear cell alignment in the direction of applied strain, as opposed to the random fiber-directed adhesion of cells on control scaffolds. Though alternatively, mechanical loading may also enhance nutrient diffusion through the culture medium and promote cell survival over the unloaded groups. Notably, however, a consistently greater number of cells were measured on aligned scaffolds at all time points after day 1, suggesting that linear matrix alignment may promote greater cell density on scaffolds.

Total matrix deposition by MSCs was found to increase significantly with tensile stimulation on both aligned and unaligned nanofiber scaffolds. These observations corroborate previous reports of elevated MSC biosynthesis on PCL nanofibers in response to both tensile and chemical stimuli [44], as well as for human fibroblasts cultured on polyurethane nanofibers [45] and subjected to tensile strain. However, in contrast to these reports, the results of this study reveal that mechanical stimulation alone can enhance MSC biosynthesis, with significantly higher per-cell collagen production on both

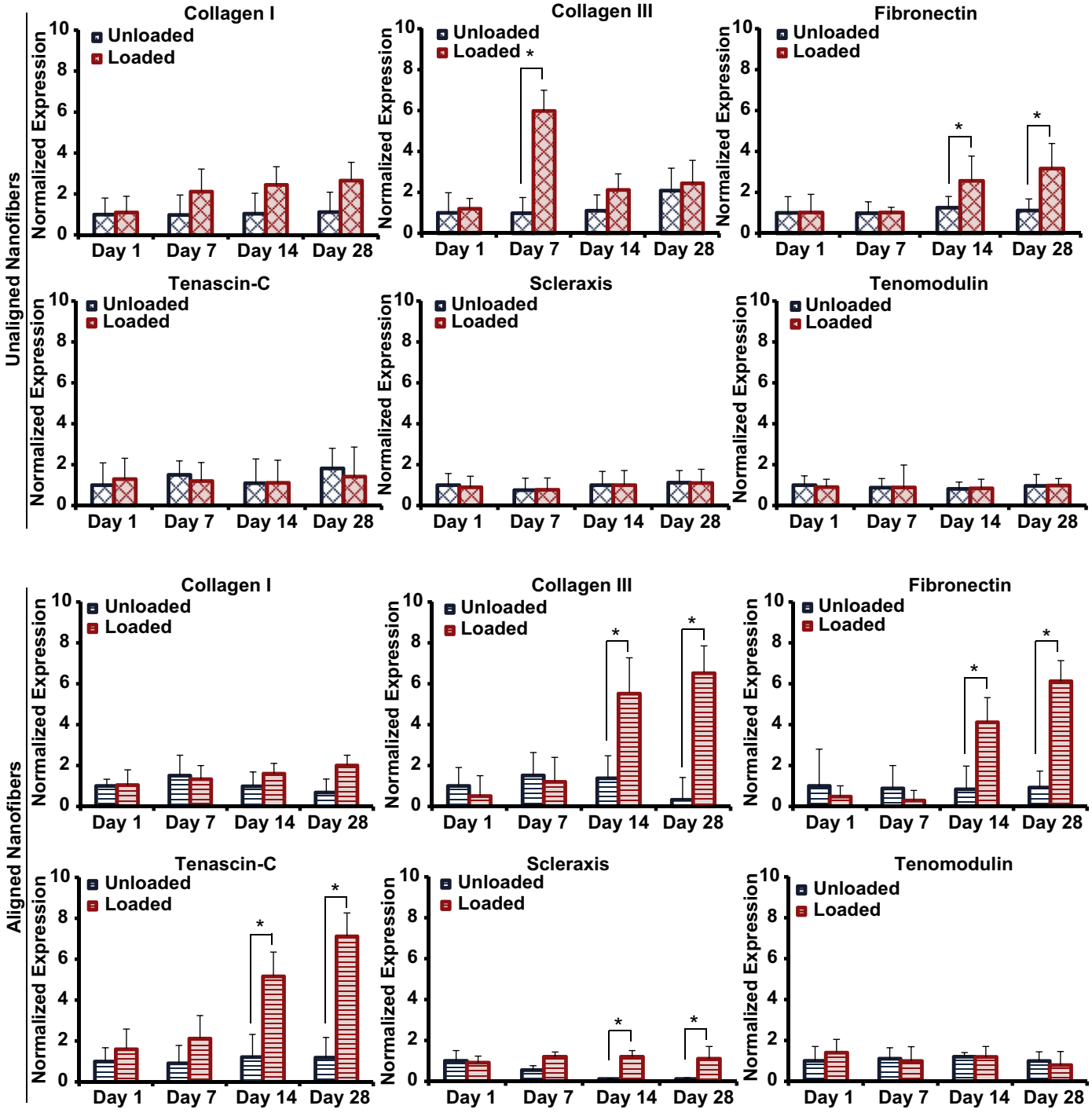

Fig. 5. *Cell Differentiation*. The expression of fibroblast-related makers by *MSCs* on unloaded and loaded scaffolds versus time (*$p < 0.05$). On unaligned scaffolds, type III collagen was upregulated after 7 days of loading but returned to control levels after 14 days. Fibronectin expression was upregulated after 14 days and remained elevated after 28 days of loading. In contrast, on aligned scaffolds, types I and III collagen, fibronectin, tenascin-C and scleraxis were all upregulated. The ratio of collagen type I:III was 8.35 ± 2.12 by cells on loaded scaffolds after 28 days of culture.

aligned and unaligned scaffolds. In addition to enhanced matrix production, the production of type III collagen by MSCs in response to tensile strain only occurs on aligned nanofibers. Type III collagen synthesis is indicative of fibroblastic differentiation as this protein represents approximately 12% (by dry weight) of the native ligament matrix [46] and provides tendons and ligaments with their strength and elasticity by forming heterotypic fibers incorporating type I collagen [47] while also playing a critical role in the healing of connective tissues [48]. These results indicate that both loading and scaffold alignment are needed to stimulate the production of type III collagen.

Analysis of MSC differentiation revealed that several key fibroblastic markers were upregulated only with the combination of nanofiber alignment and dynamic tensile loading. Though type III collagen deposition was not found on unaligned nanofibers, the observed increase in expression may arise due to the similarity of the unaligned matrix to the disorganized collagen matrix of scar tissue, as five- to ten-fold increases in type III collagen content have

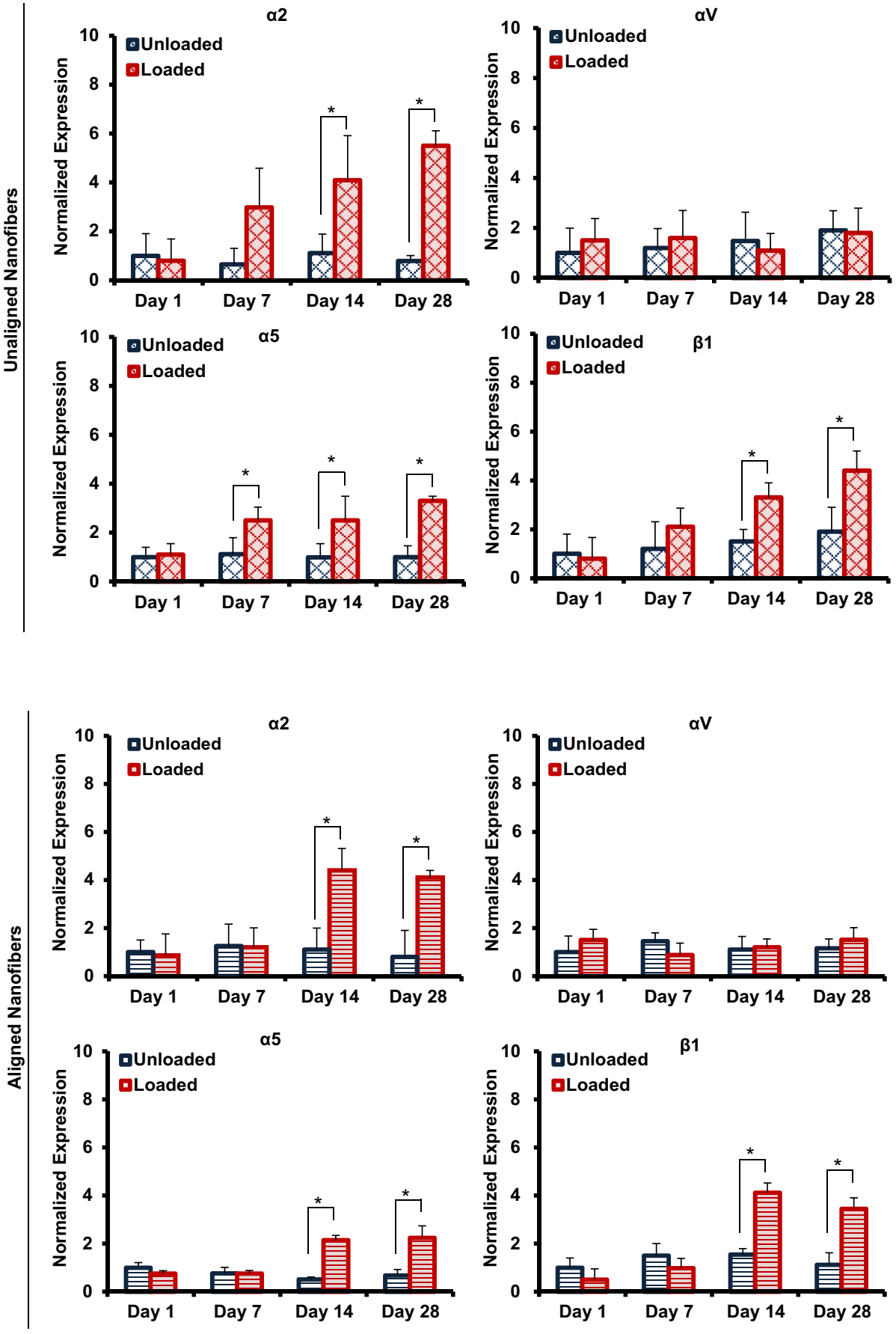

Fig. 6. *Integrin Expression.* Gene expression of integrin subunit by *MSCs* on unaligned scaffolds revealed the upregulation of integrin subunits α2, α5 and β1. (*$p < 0.05$). Similarly, on aligned scaffolds, upregulation of integrin subunits α2, α5 and β1 was observed, with differing temporal patterns as compared to those observed on unaligned scaffolds. (*$p < 0.05$).

Table 2
Summary of the effects of substrate alignment and mechanical stimulation.

Cell response	Unaligned vs. Aligned	Unaligned + Loaded	Aligned + Loaded
Cell Alignment (Fig. 3)	Aligned > Unaligned	Unaligned + Loaded > Unaligned Unaligned + Loaded = Aligned	Aligned + Loaded = Aligned Aligned + Loaded = Unligned + Loaded Aligned + Loaded > Unaligned
Cell Proliferation (Fig. 2)	Aligned > Unaligned	Unaligned + Loaded > Unaligned Unaligned + Loaded < Aligned	Aligned + Loaded > Aligned Aligned + Loaded > Unaligned + Loaded Aligned + Loaded > Unaligned
Matrix Deposition (Fig. 4)	No effect	Unaligned + Loaded > Unaligned Unaligned + Loaded = Aligned	Aligned + Loaded > Aligned Aligned + Loaded > Unaligned + Loaded Aligned + Loaded > Unaligned
Fibroblastic Differentiation (Fig. 5)	No Induction	No Induction	Induction (Col III, FN, Tenascin, and Scx) Collagen I & III deposition
Integrin Expression (Fig. 6)	No effect	Upregulated with loading	Upregulated with loading

been reported at the Achilles' tendon rupture sites during healing [49]. The changes in gene expression on aligned scaffolds are similar to those reported by Altman *et al.* who evaluated the effect of tensile strain and torsion on MSCs in type I collagen gels [2] and on silk fibers [50], reporting a similar upregulation of types I and III collagen as well as tenascin-C. Upregulation of both types I and III collagen expression is also in agreement with the increase in total collagen deposition as well as the production of type III collagen by MSCs on aligned scaffolds in response to loading. Additionally, as no specific marker serves to distinguish ligament fibroblasts from other fibroblasts present in connective tissues, the type I:III collagen ratio is an important indicator of cell phenotype as it varies significantly between ligaments (~7:1) and tendons (~20:1) [46] and is substantially decreased in scar tissue (~1:1) [51]. In this study, cells on unaligned scaffolds measured a collage I:III ratio of 0.51 ± 1.26 without loading and 1.03 ± 0.99 with loading. In contrast, cells on aligned scaffolds measured a ratio of 8.35 ± 2.12 after 28 days of loading, as opposed to approximately 2.07 ± 1.11 for the unloaded group, thereby suggesting that cells assumed a ligament fibroblast-like phenotype in response to mechanical stimulation only on the aligned nanofibers.

Furthermore, scleraxis, a transcription factor that has been shown to be critical for tendon and ligament formation during development in both avian and murine models [52,53], was maintained on scaffolds subjected to mechanical stimulation while decreasing in unloaded scaffolds, a trend similar to that reported by Kuo *et al.* who used a collagen gel system seeded with human MSCs [54]. However, tenomodulin, a transmembrane glycoprotein induced by scleraxis and implicated in collagen organization [55,56], was not upregulated with stimulation in this study. Tenomodulin, a late marker of tendon and ligament formation, is regulated by scleraxis [55] and is likely to be upregulated in long term culture.

In addition, mechanical stimulation, on both substrates, leads to significant changes in integrin expression with different temporal patterns, indicating that these receptors mediate mechanotransduction. Integrin upregulation has also been observed for MSCs loaded in torsion on silk fibers, whereby a significant increase in α2 expression was found albeit without a concurrent upregulation of β1 [57]. The elevated expression of these integrins is likely in response to loading, ensuring that there are sufficient numbers of surface receptors to translate the physical stimulation. The biomimetic aligned scaffold, which resembles the native collagenous ECM, may also contribute to the observed increase in α2 expression as the β1 subunit complexes with α2 to bind to collagen [58]. However, no upregulation in α2 expression was observed for MSCs on unaligned or aligned scaffolds in the absence of loading, indicating that for MSCs, α2 upregulation is linked primarily to mechanical stimulation. Further, the α5 integrin complexes with β1 to bind to fibronectin [59] and has been demonstrated to be upregulated by MSCs upon binding to fibronectin functionalized surfaces [60,61]. The concomitant increase in fibronectin expression observed here may be coupled with the upregulation of these integrins as fibronectin plays a central role in cell adhesion and also can influence a variety of downstream pathways. For example, binding to the α5β1 receptor has been shown to activate the Shc pathway which promotes cell proliferation and is potentially responsible for the observed increase in cell number on scaffolds subjected to mechanical stimulation this study [62]. The downstream effects of these cell–matrix interactions will be investigated in future studies.

The findings of this study have broad implications for scar-less wound healing and guided soft tissue repair. All three of the integrin subunits upregulated in this study have been implicated in ligament and tendon injury response [59]. The α2β1 integrin, specifically, is known to be utilized by cells to contract collagen fibrils during matrix reorganization and wound healing [63], and the upregulation of these integrins suggest a nanofiber-driven matrix remodeling response by these stem cells. In addition, by modulating alignment, the nanofiber matrix can be used to model both the healthy tissue (aligned) and a disorganized wound site (unaligned) during repair. Moreover, the ability of mechanical loading to 'rescue' cell alignment toward a more physiologically relevant organization may be significant. However, the lack of fibroblastic differentiation by MSCs on either the statically cultured unaligned or aligned substrate indicates that neither mechanical loading nor substrate alignment alone is sufficient to drive MSCs toward a fibroblastic phenotype, thereby demonstrating that *both* biomimetic architecture and physiologic mechanical stimulation are needed to control MSC differentiation and guide tissue healing without the addition of growth factors. Clinically, it is envisioned that a strategy of concurrent stimulation with a biomimetic matrix and physiological loading could be utilized to direct the differentiation of MSCs on scaffolds for connective tissue engineering as well as extended applications in scar-less wound repair. Future work will investigate the effects of cellular deformation on the aligned and unaligned nanofiber scaffolds while also further optimizing the loading regimen for both differentiation and matrix production.

5. Conclusions

This study investigates the coupled effects of nanofiber matrix alignment and mechanical stimulation on stem cell differentiation. The MSCs differentiate into ligament fibroblast-like cells when cultured on aligned nanofibers and subjected to tensile loading. In contrast, on unaligned nanofibers, mechanical loading only modulates cell attachment morphology without subsequent induction of fibroblastic differentiation. These results demonstrate

the deterministic role biomaterial substrate alignment plays in stem cell response to mechanical loading, as both biomimetic alignment and tensile loading are required for the induction of MSCs into ligament fibroblasts.

Conflicts of interest

All authors have no conflicts of interest.

Disclosures

The authors indicate no potential conflicts of interest.

Acknowledgments

The authors would like to thank Gregory M. Fomovsky, Ph.D., Jeffrey Holmes, Ph.D, and Kevin D. Costa, Ph.D. for use of the Fiber3 circular statistical analysis software. In addition, the authors would like to thank Keith Yeager for assistance with bioreactor fabrication and Barclay Morrison, Ph.D. for use of the flow cytometer. This study was supported by the National Institutes of Health (R21-AR056459, R01-AR055280), the National Science Foundation (Graduate Research Fellowship, SDS) and the New York State Stem Cell ESSC Board (NYSTEM).

References

[1] Pittenger MF, Mackay AM, Beck SC, Jaiswal RK, Douglas R, Mosca JD, et al. Multilineage potential of adult human mesenchymal stem cells. Science 1999; 284(5411):143–7.
[2] Altman GH, Horan RL, Martin I, Farhadi J, Stark PR, Volloch V, et al. Cell differentiation by mechanical stress. FASEB J 2002;16(2):270–2.
[3] Prockop DJ. Marrow stromal cells as stem cells for nonhematopoietic tissues. Science 1997;276(5309):71–4.
[4] Darby IA, Hewitson TD. Fibroblast differentiation in wound healing and fibrosis. In: Kwang WJ, editor. International review of cytology a survey of cell biology, vol. 257. Academic Press; 2007. p. 143–79.
[5] da Silva Meirelles L, Caplan AI, Nardi NB. In search of the in vivo identity of mesenchymal stem cells. Stem Cells 2008;26(9):2287–99.
[6] Alhadlaq A, Mao JJ. Mesenchymal stem cells: isolation and therapeutics. Stem Cells Dev 2004;13(4):436–48.
[7] Langer R, Vacanti JP. Tissue engineering. Science 1993;260(5110):920–6.
[8] DiGirolamo CM, Stokes D, Colter D, Phinney DG, Class R, Prockop DJ. Propagation and senescence of human marrow stromal cells in culture: a simple colony-forming assay identifies samples with the greatest potential to propagate and differentiate. Br J Haematol 1999;107(2):275–81.
[9] Yoshimoto H, Shin YM, Terai H, Vacanti JP. A biodegradable nanofiber scaffold by electrospinning and its potential for bone tissue engineering. Biomaterials 2003;24(12):2077–82.
[10] Garreta E, Gasset D, Semino C, Borros S. Fabrication of a three-dimensional nanostructured biomaterial for tissue engineering of bone. Biomol Eng 2007;24(1):75–80.
[11] Baker BM, Mauck RL. The effect of nanofiber alignment on the maturation of engineered meniscus constructs. Biomaterials 2007;28(11):1967–77.
[12] Nerurkar NL, Elliott DM, Mauck RL. Mechanics of oriented electrospun nanofibrous scaffolds for annulus fibrosus tissue engineering. J Orthop Res 2007;25(8):1018–28.
[13] Li WJ, Danielson KG, Alexander PG, Tuan RS. Biological response of chondrocytes cultured in three-dimensional nanofibrous poly(epsilon-caprolactone) scaffolds. J Biomed Mater Res A 2003;67(4):1105–14.
[14] Moffat KL, Kwei AS, Spalazzi JP, Doty SB, Levine WN, Lu HH. Novel nanofiber-based scaffold for rotator cuff repair and augmentation. Tissue Eng Part A 2009;15(1):115–26.
[15] Kumbar SG, James R, Nukavarapu SP, Laurencin CT. Electrospun nanofiber scaffolds: engineering soft tissues. Biomed Mater 2008;3(3):034002.
[16] Li WJ, Mauck RL, Cooper JA, Yuan X, Tuan RS. Engineering controllable anisotropy in electrospun biodegradable nanofibrous scaffolds for musculoskeletal tissue engineering. J Biomech 2007;40(8):1686–93.
[17] Barber JG, Handorf AM, Allee TJ, Li WJ. Braided nanofibrous scaffold for tendon and ligament tissue engineering. Tissue Eng Part A 2011. Epub.
[18] Sahoo S, Ouyang H, Goh JC, Tay TE, Toh SL. Characterization of a novel polymeric scaffold for potential application in tendon/ligament tissue engineering. Tissue Eng 2006;12(1):91–9.
[19] Sahoo S, Ang LT, Cho-Hong GJ, Toh SL. Bioactive nanofibers for fibroblastic differentiation of mesenchymal precursor cells for ligament/tendon tissue engineering applications. Differentiation 2010;79(2):102–10.
[20] Erisken C, Zhang X, Moffat KL, Levine WN, Lu H. Scaffold fiber diameter regulates human tendon fibroblast growth and differentiation. Tissue Eng Part A 2012. Accepted.
[21] Pham QP, Sharma U, Mikos AG. Electrospun poly(epsilon-caprolactone) microfiber and multilayer nanofiber/microfiber scaffolds: characterization of scaffolds and measurement of cellular infiltration. Biomacromolecules 2006; 7(10):2796–805.
[22] Murugan R, Ramakrishna S. Design strategies of tissue engineering scaffolds with controlled fiber orientation. Tissue Eng 2007;13(8):1845–66.
[23] Ma J, He X, Jabbari E. Osteogenic differentiation of marrow stromal cells on random and aligned electrospun poly(L-lactide) nanofibers. Ann Biomed Eng 2011;39(1):14–25.
[24] Skutek M, Griensven M, Zeichen J, Brauer N, Bosch U. Cyclic mechanical stretching modulates secretion pattern of growth factors in human tendon fibroblasts. Eur J Appl Physiol 2001;86(1):48–52.
[25] Schofer M, Boudriot U, Wack C, Leifeld I, Grabedunkel C, Dersch R, et al. Influence of nanofibers on the growth and osteogenic differentiation of stem cells: a comparison of biological collagen nanofibers and synthetic PLLA fibers. J Mater Sci Mater Med 2009;20(3):767–74.
[26] Jiang X, Cao HQ, Shi LY, Ng SY, Stanton LW, Chew SY. Nanofiber topography and sustained biochemical signaling enhance human mesenchymal stem cell neural commitment. Acta Biomater 2012;8(3):1290–302.
[27] Terraciano V, Hwang N, Moroni L, Park HB, Zhang Z, Mizrahi J, et al. Differential response of adult and embryonic mesenchymal progenitor cells to mechanical compression in hydrogels. Stem Cells 2007;25(11):2730–8.
[28] Grayson WL, Frohlich M, Yeager K, Bhumiratana S, Chan ME, Cannizzaro C, et al. Engineering anatomically shaped human bone grafts. Proc Natl Acad Sci U S A 2010;107(8):3299–304.
[29] Reneker DH, Chun I. Nanometre diameter fibres of polymer, produced by electrospinning. Nanotechnology 1996;7:216–23.
[30] Nathan AS, Baker BM, Nerurkar NL, Mauck RL. Mechano-topographic modulation of stem cell nuclear shape on nanofibrous scaffolds. Acta Biomaterialia 2011;7(1):57–66.
[31] De ZM, Bojsen-Moller F, Voigt M. Dynamic viscoelastic behavior of lower extremity tendons during simulated running. J Appl Physiol 2000;89(4): 1352–9.
[32] Nirmalandhan VS, Shearn JT, Juncosa-Melvin N, Rao M, Gooch C, Jain A, et al. Improving linear stiffness of the cell-seeded collagen sponge constructs by varying the components of the mechanical stimulus. Tissue Eng Part A 2008; 14(11):1883–91.
[33] Hanson AD, Marvel SW, Bernacki SH, Banes AJ, van AJ, Loboa EG. Osteogenic effects of rest inserted and continuous cyclic tensile strain on hASC lines with disparate osteodifferentiation capabilities. Ann Biomed Eng 2009;37(5):955–65.
[34] Riboh J, Chong AKS, Pham H, Longaker M, Jacobs C, Chang J. Optimization of flexor tendon tissue engineering with a cyclic strain bioreactor. J Hand Surg Am 2008;33(8):1388–96.
[35] Lu HH, Cooper Jr JA, Manuel S, Freeman JW, Attawia MA, Ko FK, et al. Anterior cruciate ligament regeneration using braided biodegradable scaffolds: in vitro optimization studies. Biomaterials 2005;26(23):4805–16.
[36] Costa KD, Lee EJ, Holmes JW. Creating alignment and anisotropy in engineered heart tissue: role of boundary conditions in a model three-dimensional culture system. Tissue Eng 2003;9(4):567–77.
[37] Wang N, Tytell JD, Ingber DE. Mechanotransduction at a distance: mechanically coupling the extracellular matrix with the nucleus. Nat Rev Mol Cell Biol 2009;10(1):75–82.
[38] Ruoslahti E. Stretching is good for a cell. Science 1997;276(5317):1345–6.
[39] Friedl G, Schmidt H, Rehak I, Kostner G, Schauenstein K, Windhager R. Undifferentiated human mesenchymal stem cells (hMSCs) are highly sensitive to mechanical strain: transcriptionally controlled early osteo-chondrogenic response in vitro. Osteoarthritis Cartilage 2007;15(11):1293–300.
[40] Bhargava MM, Beavis AJ, Edberg JC, Warren RF, Attia ET, Hannafin JA. Differential expression of integrin subunits in canine knee ligament fibroblasts. J Orthop Res 1999;17(5):748–54.
[41] Huang C, Fu X, Liu J, Qi Y, Li S, Wang H. The involvement of integrin beta1 signaling in the migration and myofibroblastic differentiation of skin fibroblasts on anisotropic collagen-containing nanofibers. Biomaterials 2012; 33(6):1791–800.
[42] Henshaw DR, Attia E, Bhargava M, Hannafin JA. Canine ACL fibroblast integrin expression and cell alignment in response to cyclic tensile strain in three-dimensional collagen gels. J Orthop Res 2006;24(3):481–90.
[43] Wang JH, Grood ES. The strain magnitude and contact guidance determine orientation response of fibroblasts to cyclic substrate strains. Connect Tissue Res 2000;41(1):29–36.
[44] Baker BM, Shah RP, Huang AH, Mauck RL. Dynamic tensile loading improves the functional properties of mesenchymal stem cell-laden nanofiber-based fibrocartilage. Tissue Eng Part A 2011;17(9-10):1445–55.
[45] Lee CH, Shin HJ, Cho IH, Kang YM, Kim IA, Park KD, et al. Nanofiber alignment and direction of mechanical strain affect the ECM production of human ACL fibroblast. Biomaterials 2005;26(11):1261–70.
[46] Amiel D, Frank C, Harwood F, Fronek J, Akeson W. Tendons and ligaments: a morphological and biochemical comparison. J Orthop Res 1983; 1(3):257–65.
[47] Waggett AD, Ralphs JR, Kwan APL, Woodnutt D, Benjamin M. Characterization of collagens and proteoglycans at the insertion of the human achilles tendon. Matrix Biol 1998;16(8):457–70.

[48] Amiel D, Kleiner JB, Roux RD, Harwood FL, Akeson WH. The phenomenon of "ligamentization": anterior cruciate ligament reconstruction with autogenous patellar tendon. J Orthop Res 1986;4(2):162–72.
[49] Eriksen HA, Pajala A, Leppilahti J, Risteli J. Increased content of type III collagen at the rupture site of human achilles tendon. J Orthop Res 2002; 20(6):1352–7.
[50] Moreau JE, Bramono DS, Horan RL, Kaplan DL, Altman GH. Sequential biochemical and mechanical stimulation in the development of tissue-engineered ligaments. Tissue Eng Part A 2008;14(7):1161–72.
[51] Murphy PG, Loitz BJ, Frank CB, Hart DA. Influence of exogenous growth factors on the synthesis and secretion of collagen types I and III by explants of normal and healing rabbit ligaments. Biochem Cell Biol 1994;72(9-10):403–9.
[52] Brent AE, Schweitzer R, Tabin CJ. A somitic compartment of tendon progenitors. Cell 2003 Apr 18;113(2):235–48.
[53] Schweitzer R, Chyung JH, Murtaugh LC, Brent AE, Rosen V, Olson EN, et al. Analysis of the tendon cell fate using scleraxis, a specific marker for tendons and ligaments. Development 2001;128(19):3855–66.
[54] Kuo CK, Tuan RS. Mechanoactive tenogenic differentiation of human mesenchymal stem cells. Tissue Eng Part A 2008;14(10):1615–27.
[55] Shukunami C, Takimoto A, Oro M, Hiraki Y. Scleraxis positively regulates the expression of tenomodulin, a differentiation marker of tenocytes. Dev Biol 2006;298(1):234–47.
[56] Docheva D, Hunziker EB, Fassler R, Brandau O. Tenomodulin is necessary for tenocyte proliferation and tendon maturation. Mol Cell Biol 2005;25(2): 699–705.
[57] Chen J, Horan RL, Bramono D, Moreau JE, Wang Y, Geuss LR, et al. Monitoring mesenchymal stromal cell developmental stage to apply on-time mechanical stimulation for ligament tissue engineering. Tissue Eng 2006; 12(11):3085–95.
[58] Garcia AJ. Get a grip: integrins in cell-biomaterial interactions. Biomaterials 2005;26(36):7525–9.
[59] Lin TW, Cardenas L, Soslowsky LJ. Biomechanics of tendon injury and repair. J Biomech 2004;37(6):865–77.
[60] Petrie TA, Capadona JR, Reyes CD, Garcia AJ. Integrin specificity and enhanced cellular activities associated with surfaces presenting a recombinant fibronectin fragment compared to RGD supports. Biomaterials 2006;27(31):5459–70.
[61] Hannafin JA, Attia EA, Henshaw R, Warren RF, Bhargava MM. Effect of cyclic strain and plating matrix on cell proliferation and integrin expression by ligament fibroblasts. J Orthop Res 2006;24(2):149–58.
[62] Giancotti FG. Integrin signaling: specificity and control of cell survival and cell cycle progression. Curr Opin Cell Biol 1997;9(5):691–700.
[63] Schiro JA, Chan BM, Roswit WT, Kassner PD, Pentland AP, Hemler ME, et al. Integrin alpha 2 beta 1 (VLA-2) mediates reorganization and contraction of collagen matrices by human cells. Cell 1991 Oct 18;67(2):403–10.